Analysis of Capacitively Coupled Chlorine-Containing Discharges

5th AEC/APC Conference
Dresden, Saxony
April 14 – 16, 2004

Gerhard Franz
University of Applied Sciences, Munich, Bavaria

- **Plasma parameters** have been simultaneously determined with LANGMUIR probes, optical emission spectroscopy, impedance measurements, and self-excited electron resonance spectroscopy
  - electrical properties: ohmic and capacitive part of a plasma, $\cos\varphi$, absorbed power
  - plasma density n_e
  - electron temperature T_e
  - electron collision frequency ν_eff
- **Derived Parameters**
  - dc conductivity
  - dc bias
  - sheath thickness
- **Softening of the plasma impedance** due to reactive gases
- **Conclusion and Outlook**

1 Etching in CCP-Discharges

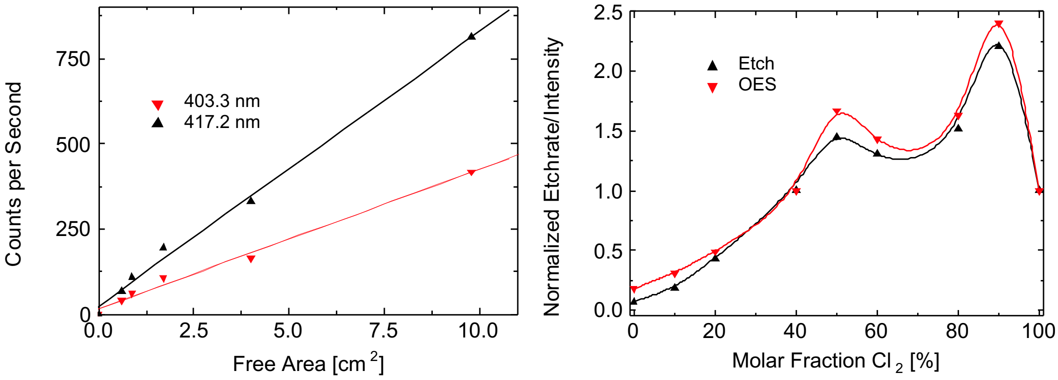

Figure 1.1. CCP-discharge of BCl_3/Cl_2: The intensity of the optical emission spectroscopy (OES) signal of Ga (4033 and 4172 Å) is proportional to the open area to be etched (LHS) [1] and almost congruent to the etch rate (RHS), shown here as functions of the molar fraction of clorine, both normalized to its value in pure chlorine [2].
H.H. Sawin, R.A. Gottscho (ER_{chem}: spontaneous etch rate, ER_{phys}: sputter rate): $ER_{\mathrm{tot}} = ER_{\mathrm{chem}} + ER_{\mathrm{phys}} + n_{\mathrm{i}} v_{\mathrm{B}} (V_{\mathrm{P}} + V_{\mathrm{DC}})$.

1. How does the characteristics of the discharge change with increasing discharge pressure and increasing power input?

2. How is the characteristics of the discharge shifted from capacitive to capacitice/resistive behavior when a strongly electronegative gas like BCl_3 is added to an electropositive gas like Cl_2 and/or Ar?

3. Do we really excite a capacitively-driven discharge in the case of strongly electronegative ambients (as is the case for Cl_2 and BCl_3), compared with argon and hydrogen which are electropositive and significantly less polarizable?

4. Is the congruent enhancement of etch rate and spectroscopic intensity of the etched species a function of plasma properties like electron density

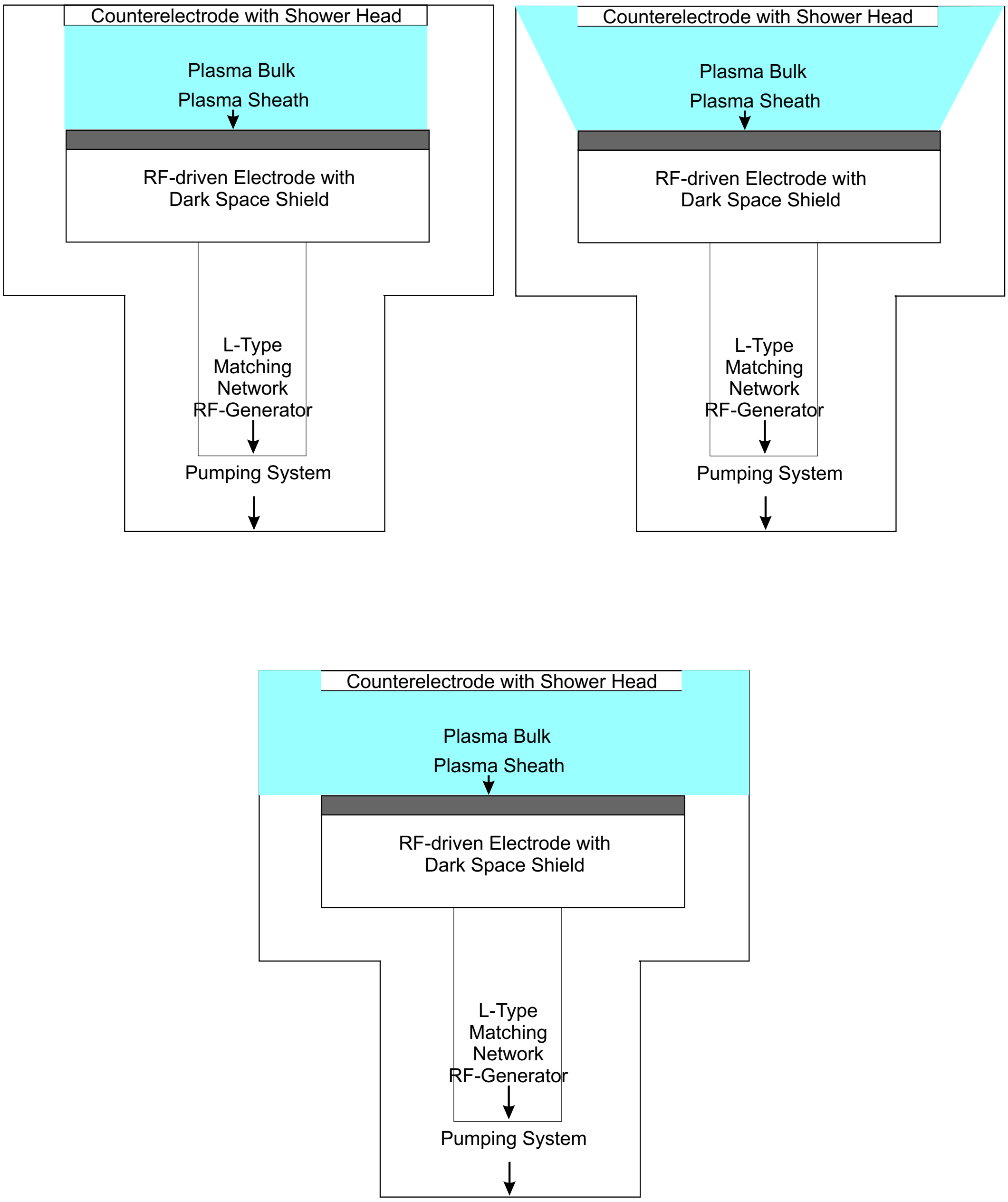

Figure 1.2. Various models for the current path. LHS seems to be realistic for a (confined) CCP discharge, whereas both the other models are valid for an ICP discharge (dependent on the plasma density).

and electron temperature, which are also responsible for the intensity of a spectral line?

5. Is the enhancement of the etch rate connected to a change of characteristics of the discharge?

2 Experimental and Model

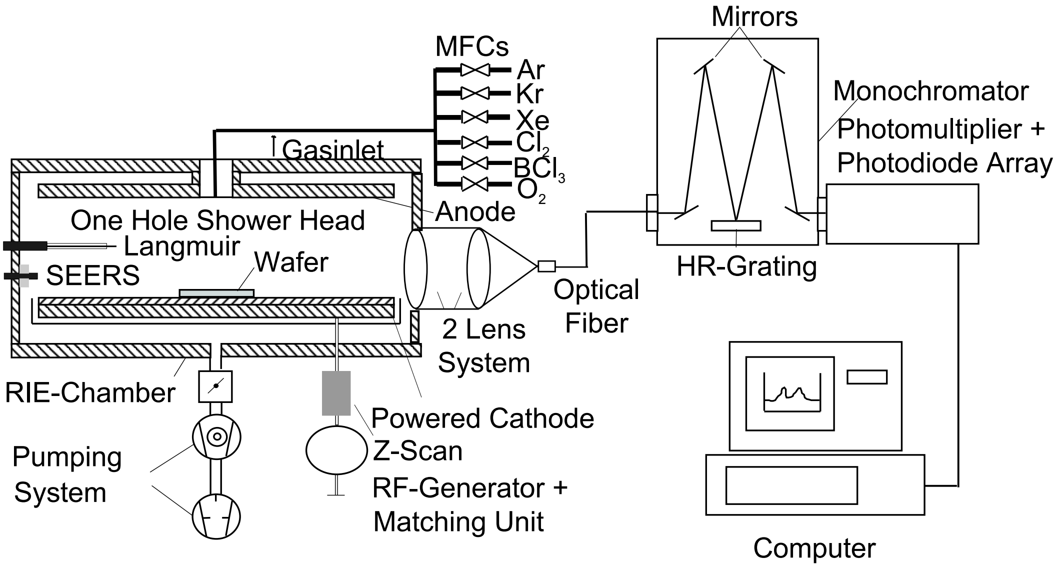

Figure 2.1. Parallel-plate reactor with plasma analytic tools: z-scan (two-port with four gates)[3]; OMA [4] [5] [6]; Langmuir and SEERS probes [7] [8] [9] [10]. PlasmaLab 90 of Oxford Plasma Technology, diameter of the hot electrode: 27.4 cm, inner diameter of the reactor: 38.0 cm, electrode gap: 5.1 cm, quartz liner: 0.6 cm [2].

Table 2.1. Plasma properties which were investigated and their evaluation methods which were applied in this study.

Plasma	*Method*			
Property	*Z-Sensor*	*Langmuir*	*OES*	*SEERS*
V_{rms}	✓			
I_{rms}	✓			
$\cos\varphi$	✓			
T_{e}		✓	✓	
n_{e}		✓		✓
V_{p}		✓		
ν_{m}				✓

TONKS, LANGMUIR, SAHA [11]:
$n_{\mathrm{P}} \propto n_{\mathrm{N}} \Rightarrow T_{\mathrm{e}} \propto 1/\ln n_{\mathrm{N}}$.
Equilibrium between energy absorbed and energy lost: n_{P}.
Equilibrium between bulk ionization and losses: T_{e}.

- Asymmetric discharge with two sheaths (high-resistive, low-capacitive at the rf-driven electrode) and the low-resistive plasma bulk.

- Plasma bulk with very low resistance, conduction is controlled by the highly mobile electrons.

$$Z^2 = R^2 + X^2. \tag{2.1}$$

$$R = V/I \times \cos\varphi \wedge Z = V/I \times \sin\varphi. \tag{2.2}$$

$$C = \frac{-\mathrm{i}}{\omega X} \wedge C = \varepsilon_0 \varepsilon \frac{A}{d_{\mathrm{sh}}} \Rightarrow\ d_{\mathrm{sh}} = \varepsilon_0 \varepsilon \omega X A \tag{2.3}$$

  with A the area of the rf driven electrode and d_{sh} the thickness of this sheath ($\varepsilon = 1$ due to the very low conductivity). For typical resistivities of some tens Ω, we obtain capacities around 100 pF.

- Stochastic heating to electrons at pressures below 75 mTorr. The thicker the sheath, the higher this amount. Sheath thickness increases with decreasing pressure and with increasing dc bias voltage (1.6 is the parametrized Bohm length, l the plasma length, n_{N} the density of the neutrals, σ the cross section for elastic collision [12]):

$$\nu_{\mathrm{eff}} \approx \frac{1.6}{l}\sqrt{\frac{V_{\mathrm{DC}}}{2\pi m_{\mathrm{e}}}} + n_{\mathrm{N}} \sigma v_{\mathrm{e}}. \tag{2.4}$$

- Neglect of γ processes (no production of secondary electrons due to reactions of hot ions and electrons with surfaces).
- The self-bias is closely connected to the effective power which is transmitted into the plasma [13]:

$$V_{\mathrm{dc}} = X\sqrt{\frac{P}{R}}. \tag{2.5}$$

3 Electrical Behavior

3.1 Absorbed Power vs. Radiated Power

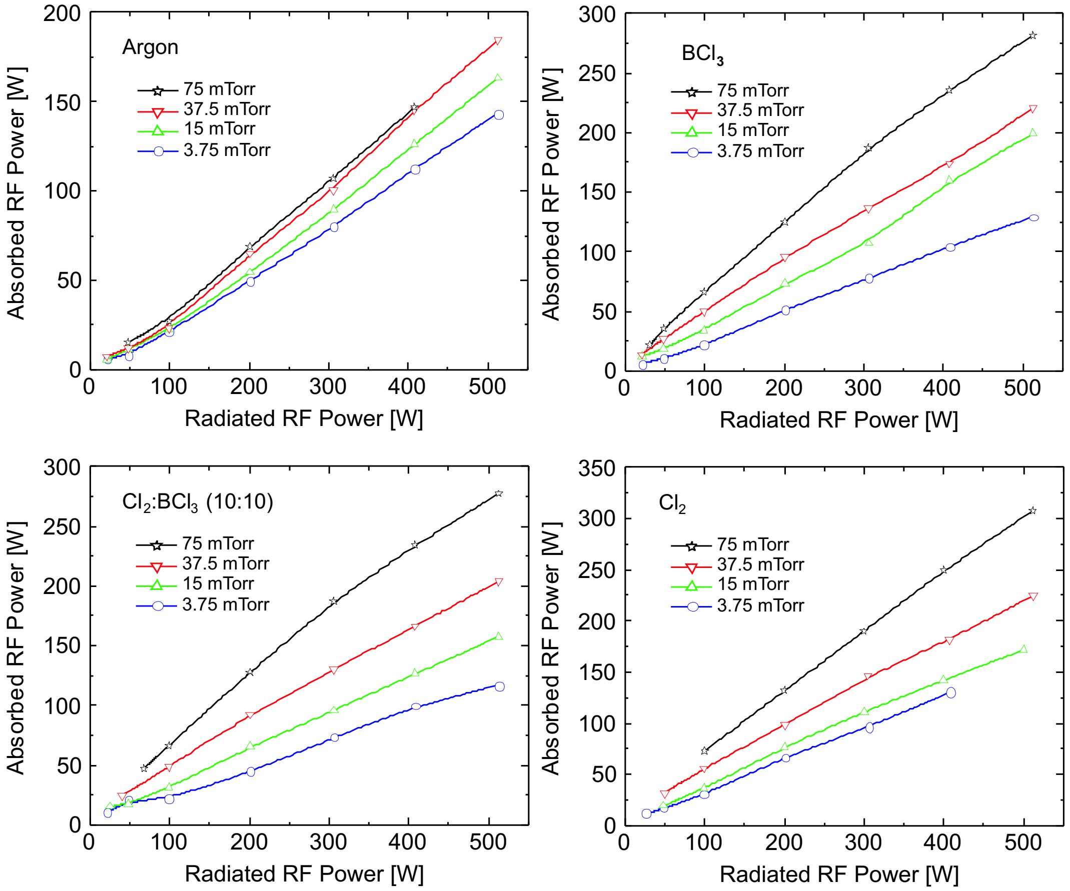

Figure 3.1. Absorbed power vs. emitted power for four different discharges, arranged with less capacitive character. In argon, significantly less than half the emitted power is absorbed, for chlorine, it is more than 60, to higher pressures 70 %. Hence it is the nature of the gas and not only stray capacitancies ...

3.2 Impedance Characteristics

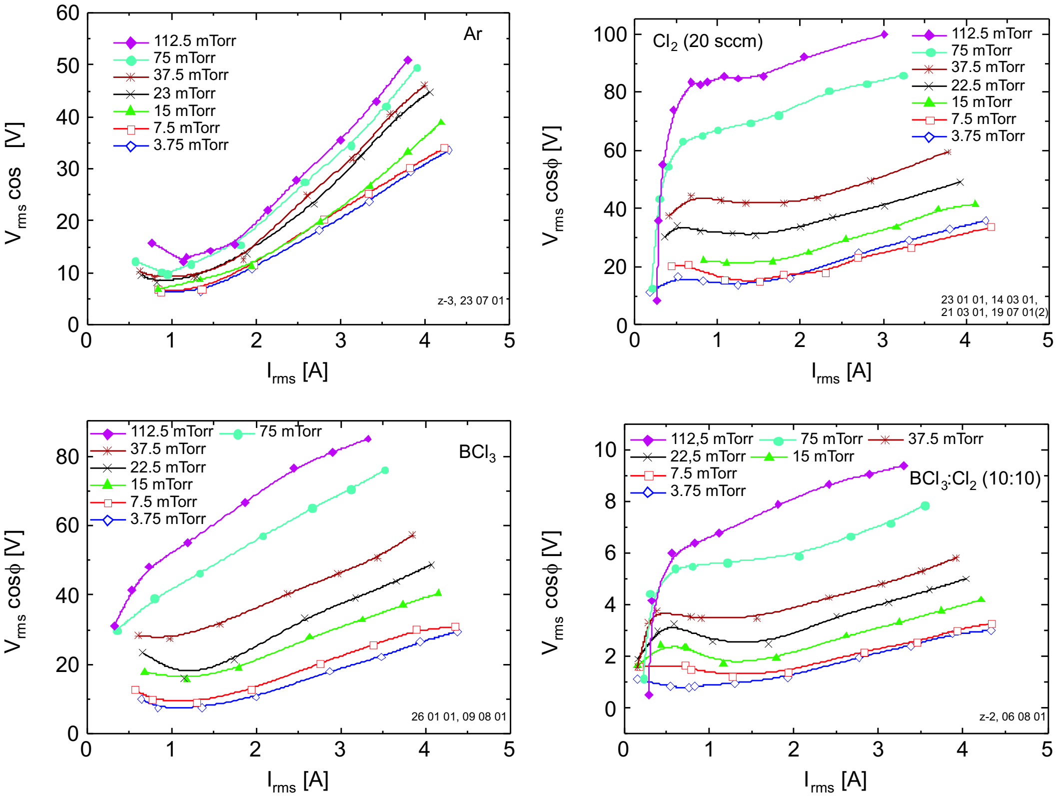

Figure 3.2. Real part of the discharge voltage for argon, chlorine, boron trichloride and the 1:1 mixture of chlorine and boron trichloride.
- At low pressures (below 20 mTorr) we observe a nearly constant (positive) slope for $V \cos\varphi$, to which sometimes a second component is added at low currents.
- For Ar, BCl_3 and the 1:1 mixture of Cl_2 and BCl_3, this component is strong enough to lead to a negative slope for the $V \cos\varphi$ vs. I curve.
- For the highest discharge pressures in Cl_2 and Cl_2-containing mixtures, the character of the discharge at low discharge currents is extremely non-capacitive (leading to power factors up to 0.9).

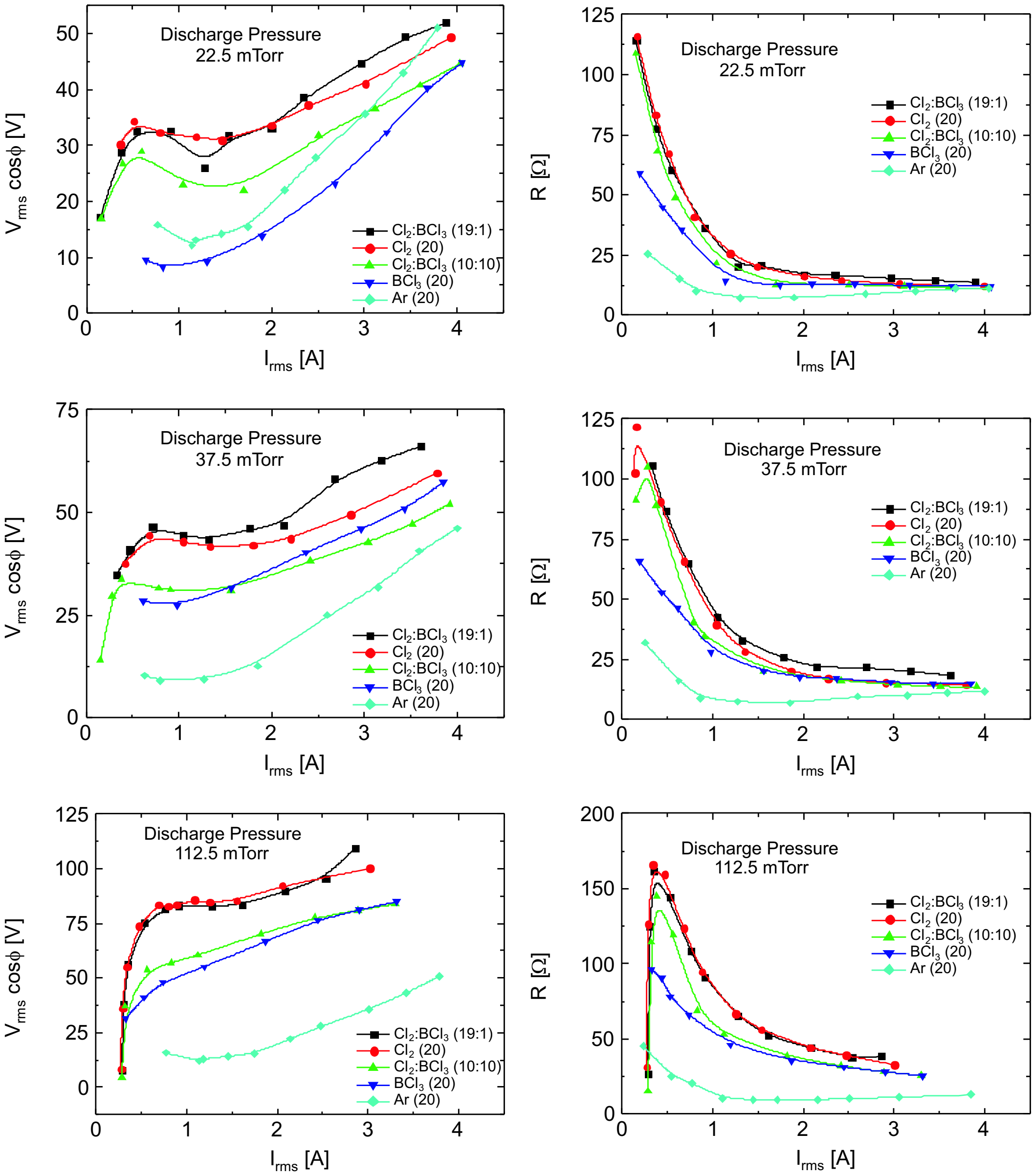

Figure 3.3. Up to pressures of 22.5 mTorr, all Cl-containing gas mixtures behave as argon. The transition starts between 22.5 and 37.5 mTorr.
The higher the real part of the resistance, the higher the ohmic component, the higher the ionic conduction current. The absorption of electric power is improved by enlargening $V_{\mathrm{rms}} \cos\varphi$. This effect is significantly stronger than the simultaneous enhancement of the real part of the resistance.

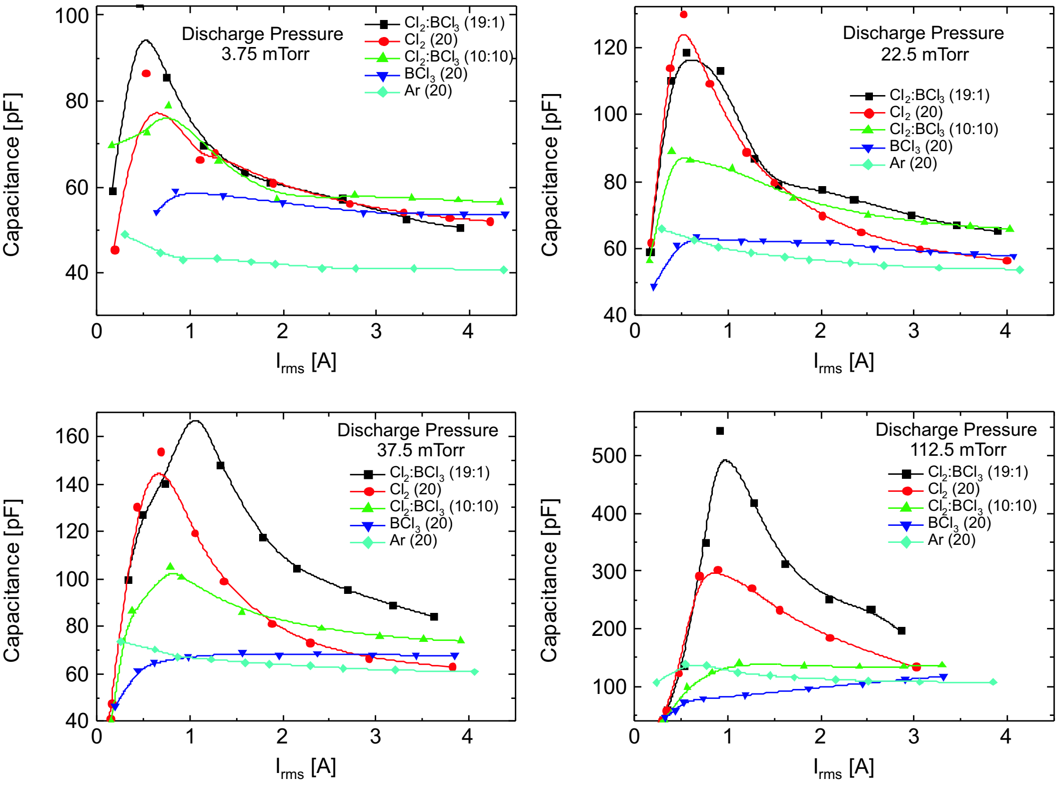

Figure 3.4. Capacitance (imaginary part of the resistance) in discharges of argon, chlorine, boron trichloride and some mixtures. Assuming pure capacitive character non-collisional characteristics, and thickness control rather by the rf voltage than by the DEBYE length, the calculated thickness for the electrically defined sheath is some mm. These values are used to calculate the thickness of the electrically defined sheath thickness. These values are also employed for the self-consistent analysis of the electrical conductivity (combination of electrical measurements, SEERS and Langmuir probe analysis.

4 Plasma Electron Density and Temperature

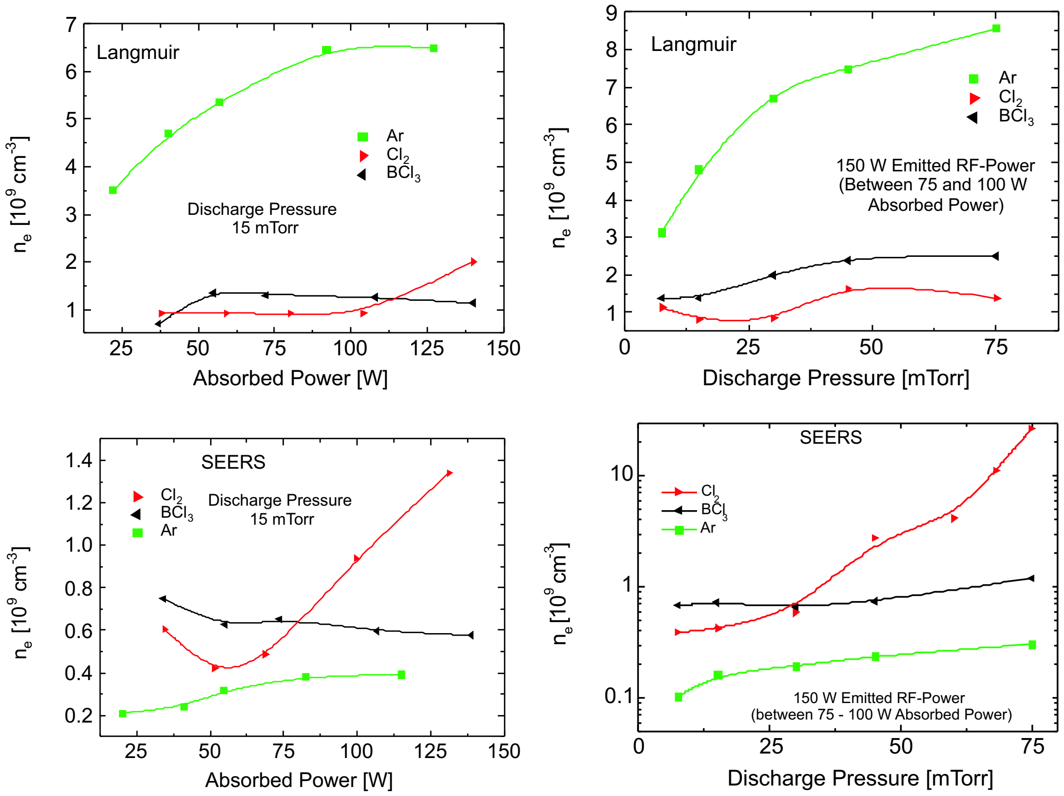

Figure 4.1. The electron plasma density n_e TONKS and LANGMUIR: equilibrium between the energy absorbed from the electromagnetic field and energy loss) as function of emitted RF power and discharge pressure (Langmuir and SEERS).

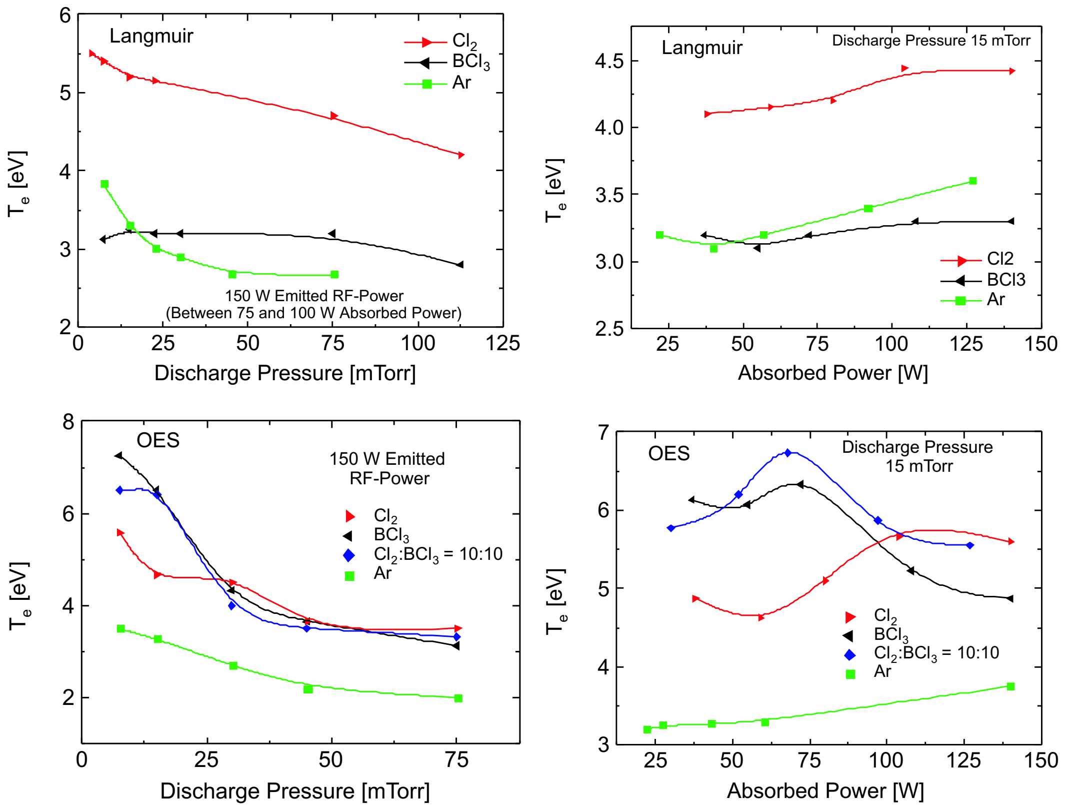

Figure 4.2. Electron temperature (Langmuir and OES) as function of discharge pressure at constant emitted RF power of 150 W (LHS) and RF power (RHS, at constant discharge pressure of 2 Pa = 15 mTorr), in discharges of Ar, Cl_2 and BCl_3.
LANGMUIR: Pressure-dependence: hyperbolic behavior for Ar, linear drop for Cl_2, relatively weak, but decreasing dependence for BCl_3.
Power-dependence: slight increase over the whole range for Ar and Cl_2, T_e for BCl_3 remains constant over the whole power range. BCl_3 reminds much more an inert gas than Cl_2.
OES: The electron energy is highest in the BCl_3 containing atmospheres, followed by chlorine, but significantly lowest in argon. $\mathcal{EEDF}$ is assumed Maxwellian.
Whereas the shape for the $T_e(p)$ curves is nearly the same for OES and Langmuir, and also the values for Ar are the same within ±5%, this is definitely not the case for the molecular gases which are calculated to be much hotter by OES. Since in ICP discharges, the difference is much smaller [14], this must be due to the lower electron density which prevents a good electronic thermalization [15].

5 Bulk Temperature and Collision Frequency

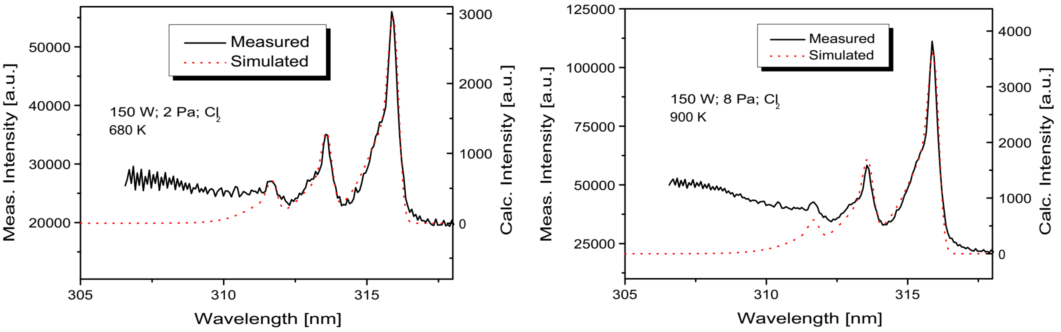

Figure 5.1. Determination of the gas temperature with rotational spectroscopy of nitrogen bands and their simulation [16]: $C^3\Pi \rightarrow B^3\Pi$ (315.93 nm: v': 1, v'': 0; 313.6 nm: v': 2, v'': 1). T_{gas} from 680 K at 2 Pa and 150 W to 925 K at 10 Pa and 150 W (Δ: 40 %); or 800 K at 400 W and 2 Pa (Δ: 20 %). According to ideal gas law, the number density is reduced by the inverted factor, and since the pressure is downstream-controlled, we should correct the indicated pressure by this (further interpolated) factor.

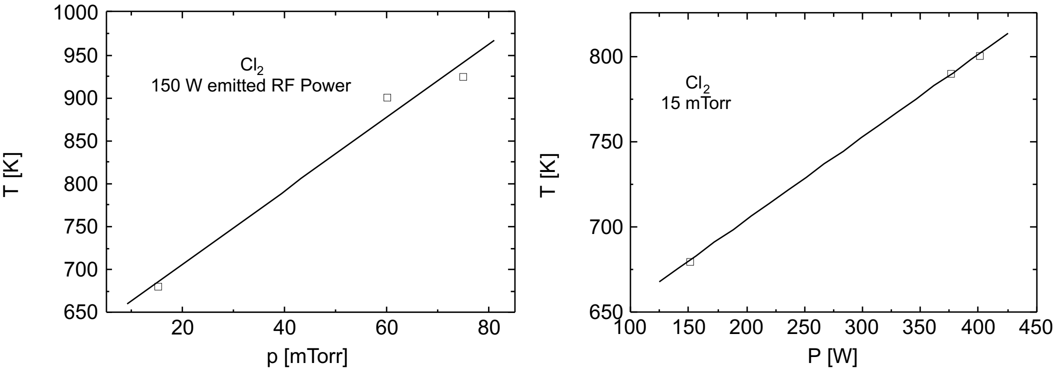

Figure 5.2. Gas temperature as function of discharge pressure at constant emitted RF power (150 W = 0.3 W/cm^2, LHS) and of emitted RF power at constant discharge pressure (15 mTorr or 2 Pa) in discharges of Cl$_2$.

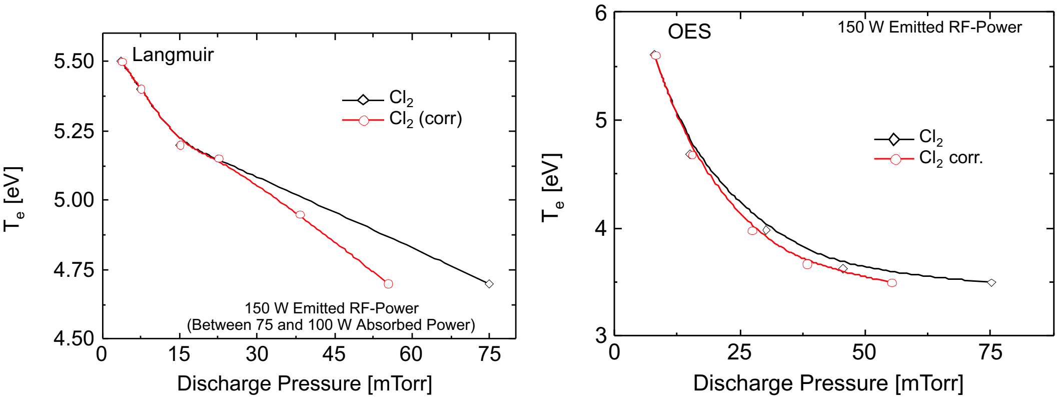

Figure 5.3. Only at high pressures (more than 40 mTorr), a correction due to lower gas densities is necessary. here shown for pure chlorine.

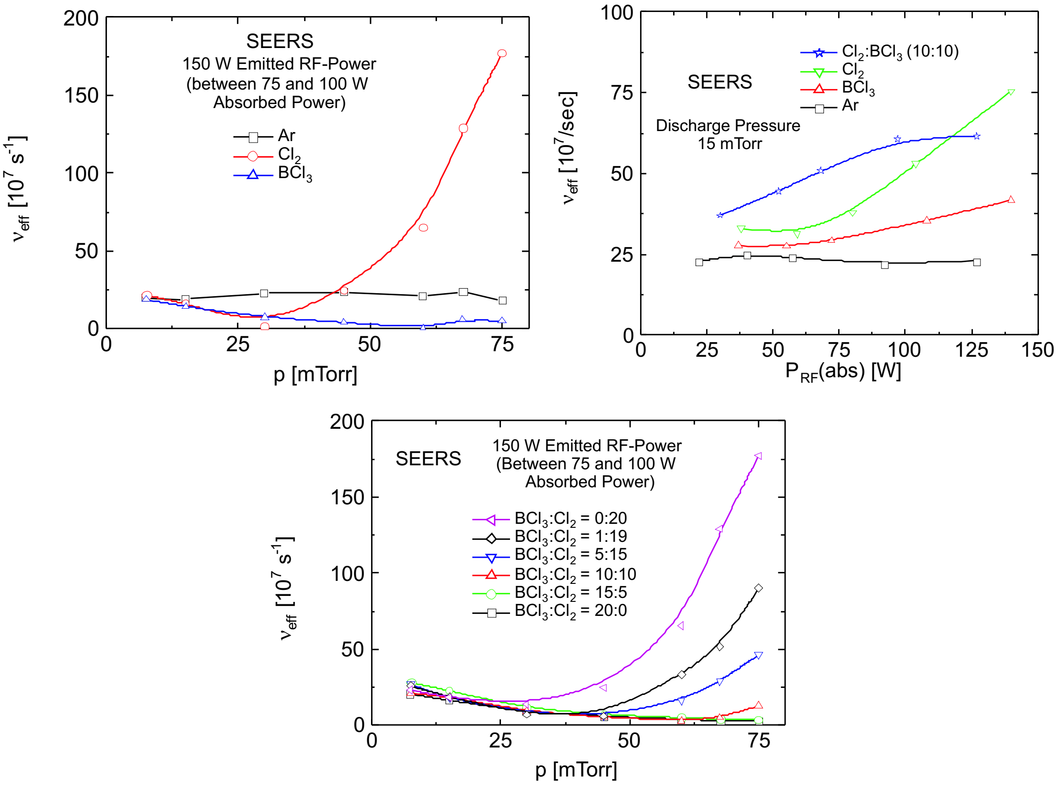

Figure 5.4. ν_{eff} as function of discharge pressure at an emitted RF power of 150 W in discharges of Ar, Cl_2 and BCl_3 (LHS) and mixtures of BCl_3 and Cl_2 (RHS). BCl_3 and Ar remain in the regime of stochastic heating, whereas Cl_2 changes gradually to ohmic heating at about 35 mTorr ($\nu_{\text{m}} \propto n_{\text{N}}$). There is only a slight dependence of ν_{eff} on absorbed rf power (below). Stepwise dilution of Cl_2 with BCl_3 leads to a continuous transition to the stochastic regime.

6 Derived Properties

6.1 Sheath Thickness

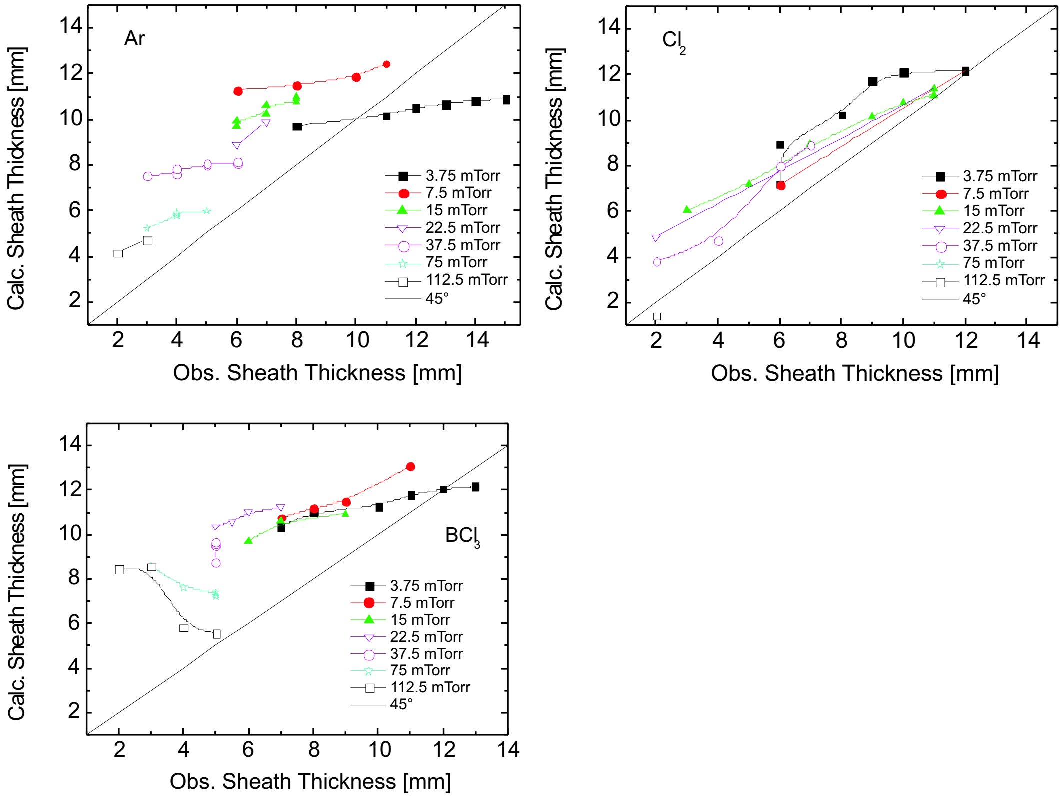

Figure 6.1. d_{sh}, as calculated using the capacitor formula $d_{\text{sh}} = \varepsilon_0 \omega A \omega X$, compared with direct observations of the sheath thickness. $d_{\text{sh}} \propto V_{\text{DC}}$. For high pressures and high voltages in reactive gases, opposite behavior is observed! Following Godyak [17], the thickness as observed with the naked eye is the border of the oscillating sheath, whereas the electrically defined thickness is the mean value of the sheath border.

6.2 DC Electrical Conductivity

- Electric measurements:
  - Real part R of the impedance Z;
  - c obtusely cone-shaped as evaluated with LANGMUIRprobe measurements (c will be modified from $l/\pi r_1^2$ to $l/\pi r_1 r_2$, σ will decrease in this volume to $^1\!/_3$);
  - $\Rightarrow \rho \wedge \sigma$.
- SEERS measurement:
  - SEERS: $\frac{n_\mathrm{p}}{\nu_\mathrm{eff}}$.
  - $\sigma = \frac{n_\mathrm{p} e_0^2}{m_\mathrm{e} \nu_\mathrm{eff}} = 0.28 \times 10^{-7} \frac{\mathrm{Coul}^2}{\mathrm{kg}} \frac{n_\mathrm{e}}{\nu_\mathrm{m}}$.
  - Neglect of amount of heavy ions due to their low mobility.

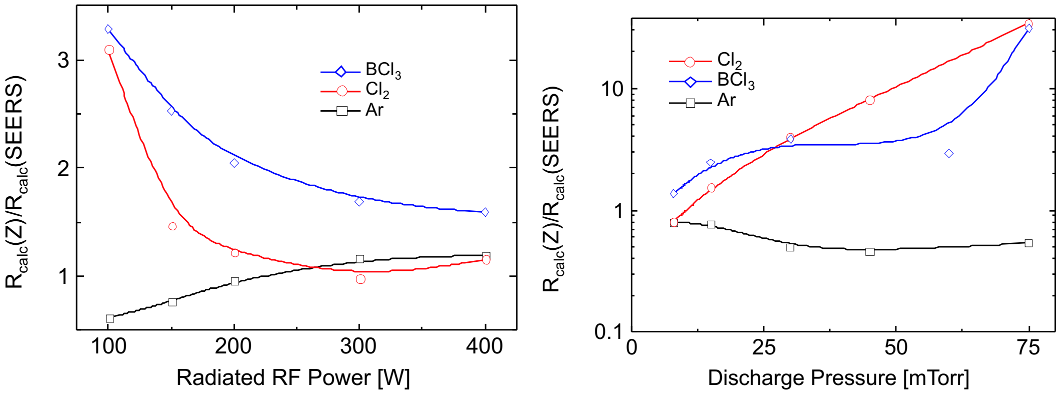

Figure 6.2. Comparison of the real part of the impedance, R, measured with a Z-scan and measured with SEERS, assuming the validity of the free electron model (hydrodynamic approach) with cone-shaped cell constant. The concordance is best(± 10 %) for real capacitive plasmas, *i. e.* $\cos\varphi \longrightarrow 0$ (low pressures, high power), since the evaluation procedure of SEERS is based on this assumption.

6.3 DC Bias

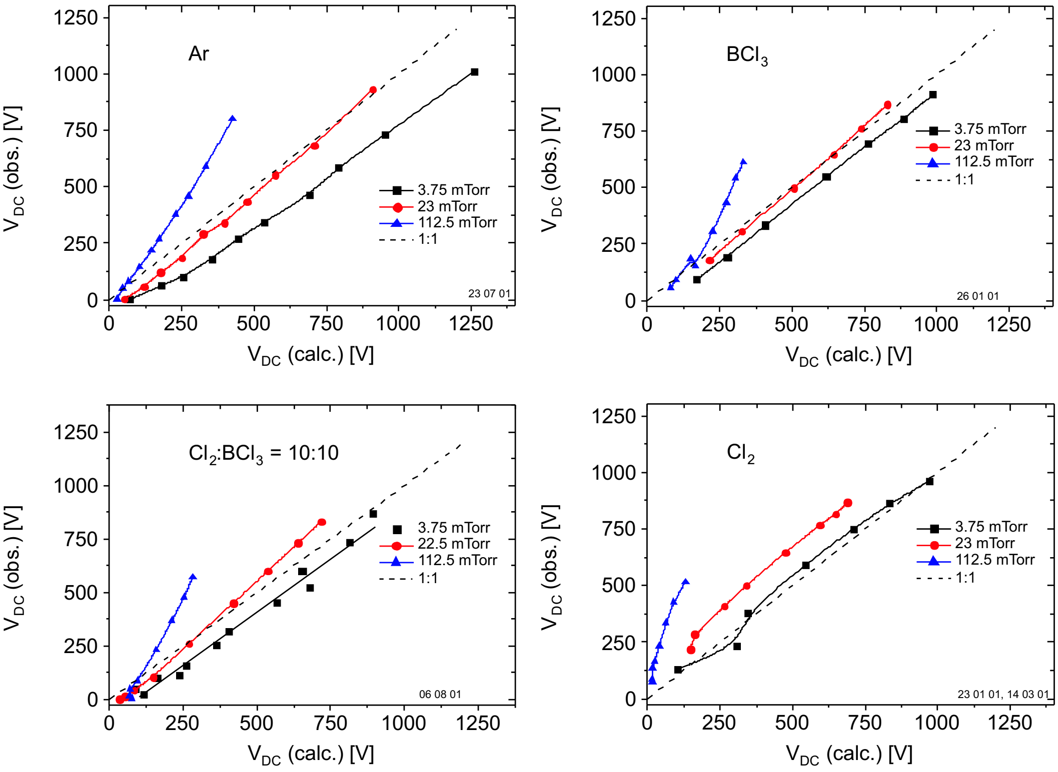

Figure 6.3. Comparison of the measured dc bias voltage with the calculated value according to a highly asymmetric discharge with series configuration of sheath and plasma bulk:
$V_{\mathrm{DC}} = X\sqrt{\frac{P}{R}}$.
For a perfect working model, the 1:1 line is expected. The deviations are due to the increasing dc conductivity of the sheath. The higher this tendency the lower the pressure for perfect concordance with the model.

7 Conclusion

The behavior of the bulk plasma of BCl_3 and Cl_2 and their mixtures in capacitively-coupled discharges has been evaluated employing the methods Langmuir probe, optical emission spectroscopy, and self-excited electron resonance spectroscopy, along with electrical measurements of the characteristics of the discharge, and compared and calibrated with argon.

- At high powers and low pressures, the discharge tends to be capacitive, *i. e.* the rf power is completely dissipated into electron heating (collisional and stochastic); nearly no power dissipation takes place in the sheath for ion acceleration by the rectified dc sheath voltage [17].

- The **power input** in inert gases is worse than in reactive, molecular gases due to the possibility of excitation of internal grades of freedom (≤ 50 % in Ar, ≥ 70 % in Cl_2.

- The **power factor** $\cos\varphi$ is zero at low pressures and high powers to increase to 1 at high pressures and low powers for Cl_2. The power factor for chlorine is typical double the value of boron trichloride.

- Ar is "harder" than BCl_3 than Cl_2.

- BCl_3 and Cl_2 are **Lewis acids.** The 1:1 mixture of chlorine and boron trichloride is supposed to exhibit some chemical effects (LEWIS acid) which dominate the electrical behavior of the real part of the voltage/current relation. Both chlorine and boron trichloride are expected to generate negative ions, especially the latter which is counted to the strongest Lewis acids. However, this investigation reveals the electropositive character of pure BCl_3 which behaves in several ways as Ar. **Only in mixtures with Cl_2 its character as Lewis acid is visible.**

- Below discharge pressure of 25 mTorr, *both the gases Cl_2 and BCl_3 (and consequently their mixtures) do not exhibit electronegative behavior.*

- $\boldsymbol{n}_{\mathbf{e}}$
  - SEERS delivers data one orders of magnitude lower than LANGMUIR.
  - n_e is significantly reduced compared to Ar.

- $\boldsymbol{T}_{\mathbf{e}}$
  - Hyperbolic pressure dependence only for OES, but are very high at low pressures.
  - T_e is significantly higher than in Ar.
  - Variation of $\mathcal{EEDF}$ MAXWELLian or DRUYVESTEYNian does shift the T value only by an additive amount.

- $\boldsymbol{\nu}_{\mathbf{m}}$ does not show a large variation, except for Cl_2 at high discharge pressures. This is referred to the overlap of the regimes of stochastic heating and OHMic heating.

- $\boldsymbol{T}_{\mathbf{bulk}}$ is determined by rotational electron excitation spectroscopy (N_2 added to Cl_2). There are corrections of up to 30 % at 75 mTorr (55 mTorr).

- **The increase in etch rate by more of a factor of 2 when adding some BCl_3 to chlorine cannot be explained by "physical" measurements.**

- Most remarkable are **Islands of Stability**: for certain regions of RF power and discharge pressure, a plasma property like n_e is nearly constant. This can be seen best for the pressure dependence of the collision frequency ν_eff which is constant over nearly the whole range for Ar and BCl_3 which are still in the regime of stochastic electronic heating, and the lower pressure range for Cl_2. Above 35 mTorr, electronic ohmic heating competes with the latter mechanism. Also, the real part of the plasma resistance remains constant over some amperes of discharge current.

Bibliography

[1] G. Franz; Spring Meeting of the Electrochemical Society, Seattle, Wash., 1999

[2] G. Franz; J. Vac. Sci. Technol. **A 16**, (1998)

[3] B. Andries, G. Ravel, and L. Peccoud; J. Vac. Sci. Technol. **A 7**, 2774 (1989)

[4] M.V. Malyshev, V.M. Donnelly; J. Vac. Sci. Technol. **A 15**, 550 (1997)

[5] J. Kaindl, S. Sotier, and G. Franz; J. Electrochem. Soc. **142**, 2418 (1995)

[6] G. Franz, Ch. Hoyler, and J. Kaindl; J. Vac. Sci. Technol. **B 14**, 126 (1996)

[7] M. Klick; J. Appl. Phys. **79**, 3445 (1996)

[8] M. Klick; Phys. Rev. **47**, 591 (1993)

[9] M. Klick, and W. Rehak; 12th Internat. Sympos. Plasma Chem., Aug 21 – 25, 1995, Univ. of. Minnesota, Minneapolis, Minn., Proc., p. 510

[10] M. Klick, M. Kammeyer, W. Rehak, W. Kasper, P. Awakowicz, and G. Franz; Surf. Coat. Technol. **98**, 1395 (1998)

[11] L. Tonks, I. Langmuir; Phys. Rev. **34**, 876 (1929)

[12] M. Klick, unpublished results

[13] A.P. Paranjpe, J.P. McVittie, and S.A. Self; J. Vac. Sci. Technol. **A 8**, 165 (1990)

[14] V.M. Donnelly, 49th AVS meeting, Denver, Colo., 2002

[15] T. Panagopoulos, D. Kim, V. Midha, and D.J. Economou; *Three-Dimensional Simulation of an Inductively Coupled Plasma Reactor,* J. Appl. Phys. **91**(5), 2687 (2002)

[16] K. Behringer; Plasma Phys. Control. Fusion **33**, 997 (1991)

[17] V.A. Godyak, R.B. Piejak, and B.M. Alexandrovich; IEEE Transact. Plasma Sci. **19**, 660 (1991)